



ISSN 2248-9649

International Journal of Research in Chemistry and Environment

Available online at: www.ijrce.org

Research Paper

Photocatalytic Mineralization of Azure A Using $\text{Li}_2\text{CuMo}_2\text{O}_8$ Nanoparticles

Joshi M., Kumawat P., Ameta R. and *Ameta S.C.

Department of Chemistry, PAHER University, Udaipur-313003 (Rajasthan) INDIA

(Received 29th June 2015, Accepted 25th September 2015)

Abstract: Photocatalytic mineralization of azure A was studied using lithium copper molybdate as photocatalyst. The effect of different variables like pH, concentration of dye, amount of semiconductor and light intensity was observed. The photo degradation efficiency of the catalyst for the azure A was found to be 72.08 %. Under optimal conditions the rate constant k was $2.47 \times 10^{-4} \text{ sec}^{-1}$. Dye was mineralized on photocatalytic degradation into smaller ions like NO_3^- and SO_4^{2-} . Water quality parameters like pH, COD, TDS, salinity, conductivity and DO were observed before and after treatment. It was observed that photocatalytic degradation affect these parameters favourably. A tentative mechanism for photocatalytic degradation of azure A, involving OH radical as an active oxidizing species, has also been proposed.

Keywords: Azure A, Lithium copper molybdate, OH radical, Photocatalytic mineralization, Water quality parameters.

© 2015 IJRCE. All rights reserved

Introduction

Effluents from various industries like textile, pulp, paper, dyeing and printing industries contain pollutants such as acids, detergent, soaps, chemicals, pesticides, dye etc, which are the major sources of water pollution. Dye stuffs from the textile industries make the water coloured, toxic and unfit for any use. Various methods such as flocculation, coagulation, osmosis, ozonation, biological treatment etc., have been used for removing colour from waste water. Every method of wastewater treatment has its own limitation. In this context, photocatalysis has been considered as an emerging technology for the treatment of wastewater, as the photocatalysts are able to degrade the undesirable organics dissolved in water completely. The photocatalytic process can mineralize the hazardous organic chemicalsto carbon dioxide, water and simple ions.

The photocatalytic degradation of methyl orange and rhodamine 6G has been investigated by Kansal and Singh^[1] using various semiconductors such as TiO_2 , ZnO , SnO_2 , ZnS and CdS . Chakrabarti and Dutta^[2] reported that ZnO is an effective photocatalyst for the photodegradation of two model dyes: methylene blue and eosin Y while Tabatabaei

et al.^[3] carried out the removal of 4-nitrophenol (4-NP) from aqueous solution by ozone combined with nano- ZnO . Pardeshi and Patil^[4] examined the effectiveness of ZnO for photocatalytic degradation of phenol. Three types of photocatalysts Zn/ZnO , Zn/ZnO/TiO_2 and $\text{Al/Al}_2\text{O}_3/\text{TiO}_2$ were prepared by Ali et al.^[5] which were used for the degradation of pesticides cypermethrin under UV irradiation. Zhang et al.^[6] synthesized $\text{SnO}_2/\alpha\text{-Fe}_2\text{O}_3$ semiconductor for degradation of methylene blue under visible light irradiation while Kale et al.^[7] investigated ZnBiO_4 for the photodecomposition of hydrogen sulfide.

Chen et al.^[8] reported that SrTiO_3 as an effective photocatalyst for NO degradation under UV light irradiation. Bhati et al.^[9] studied the photocatalytic degradation of fast green using CeCrO_3 as photocatalyst. Huang et al.^[10] reported photodegradation of isopropanol by utilizing silver vanadate photocatalyst. The photocatalytic degradation of crystal violet using nickel containing polytungstometalate was reported by Ameta et al.^[11] Ghorai and Biswas^[12] synthesized nano-sphere TiO_2 and SrCrO_4 (SCT1) mixed oxide for photodegradation of rhodamine 6G in aqueous solution whereas Mahata et al.^[13] carried out photocatalytic degradation of some dyes with

nanosized GdCoO_3 . Sadiq and Nesaraj^[14] have carried out photodegradation of methyl orange and Rhodamin B dye using $\text{NiO-Co}_3\text{O}_4$ nano-ceramic composite. Liu et al.^[15] reported the photodegradation of rhodamine B and phenol using Cu_3SnS_4 /reduced graphene oxide (RGO) photocatalyst under UV light irradiation.

Photodegradation of dye pollutants catalyzed by $\text{g-Bi}_2\text{MoO}_6$ nanoplate, under visible light irradiation has been studied by Zhao et al.^[16] whereas Aslam et al.^[17] have carried out the photocatalytic degradation of organic pollutants using cadmium tungstate photocatalyst under UV irradiation. Chen et al.^[18] investigated photodegradation of dye pollutants catalyzed by porous $\text{K}_3\text{PW}_{12}\text{O}_{40}$ under visible light irradiation. Clark et al.^[19] reported photocatalytic activity of $\text{CaCu}_3\text{Ti}_4\text{O}_{12}$ for degradation of model organic pollutant such as methyl orange, and 4-chlorophenol. Luan et al.^[20] studied the photodegradation of methylene blue dye using Bi_2SbVO_7 and $\text{Bi}_2\text{GaTaO}_7$ as photocatalysts. Many binary and ternary oxides and sulfides have been used effectively as photocatalysts for removal of many organic pollutants, but very little work has been carried out on quaternary oxide as photocatalyst. Therefore, in the present work $\text{Li}_2\text{CuMo}_2\text{O}_8$ has been used as photocatalyst for the degradation of azure A.

Methods and Material

A quaternary oxide was prepared by method of solid-state reaction of corresponding oxides. Stoichiometric amount of Li_2CO_3 , CuO and MoO_3 were mixed and ground in an agate mortar using acetone for homogeneity. 5% solution of polyvinyl acetate in acetone was added as a binder. The sample was kept in electric muffle furnace at 300°C for 3 hrs to evaporate the binder. The sample was calcined in furnace at 650°C for 30 hrs. Then, the mixture was grind. The prepared catalyst was used for the degradation of azure A. Its IUPAC name is N', N'-dimethylphenothiazin-5-ium-3, 7-diamine chloride and molecular formula is $\text{C}_{14}\text{H}_{14}\text{ClN}_3\text{S}$. It is also called 3-amino-7-(dimethylamino) phenothiazin-5-

ium chloride and has molecular mass 291.80 g/mol. It is used in the screening test for mucopolysaccharides. The structure of azure A is given in Figure 1.

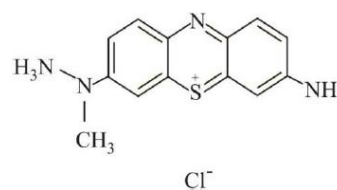


Figure 1: Structure of Azure A

1.0×10^{-3} solution of azure A (0.029 in 100 mL water) was prepared in volumetric flask with doubly distilled water and stored as a stock solution. The photocatalytic degradation of AA was observed by taking dye solution of 1.3×10^{-5} M and 0.10g of $\text{Li}_2\text{CuMo}_2\text{O}_8$ at 10 pH. Irradiation was carried out keeping the whole assembly exposed to a 200 W tungsten lamp (Philips, light intensity = 50.0 mWcm^{-2}). The intensity of light was measured with the help of a solarimeter (SM CEL 201). The pH of the solution was measured by the digital pH meter (Systronics Model 335). The desired pH of solution was adjusted by the addition of previously standardized 0.1 N sulphuric acid and 0.1 N sodium hydroxide solutions. The absorbance (A) was measured by visible absorption spectroscopy (Systronics Model 106). Some water quality parameters like pH, conductivity, salinity, TDS (Total dissolved solids), and DO (Dissolved oxygen), were determined with the help of water analyzer (Systronics Water Analyzer Model 371).

Characterization of $\text{Li}_2\text{CuMo}_2\text{O}_8$ nanoparticles:

Fourier Transform Infrared Spectroscopy (FTIR)

The infrared spectrum of the nanocomposite was recorded using Perkin Elmer-RX FTIR spectrometer model FT-IR 8400s by the KBr pellet technique in the range $400\text{-}4000 \text{ cm}^{-1}$ at a scanning rate of $1 \text{ cm}^{-1}\text{min}^{-1}$.

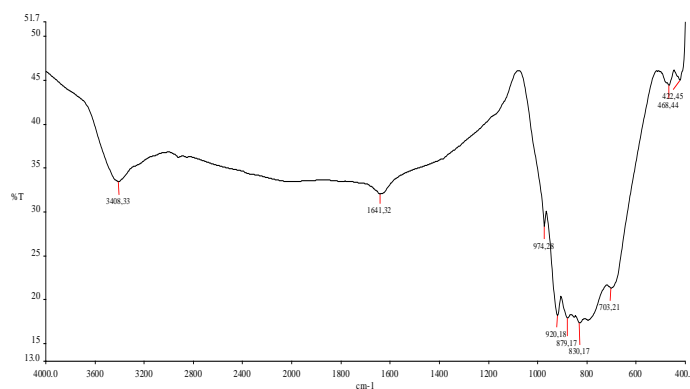


Figure 2: FTIR spectrum of lithium copper molybdate

The FTIR spectrum of $\text{Li}_2\text{CuMo}_2\text{O}_8$ is shown in Figure 2. Infrared spectroscopy is used to determine the presence of functional groups and bonds in the compound. Peaks were observed at 3408, 1641, 974, 920, 879, 830, 703, 468 and 422 cm^{-1} . The broad band around 3408 and 1641 cm^{-1} correspond to the stretching and bending mode of the hydroxyl group of absorbed water^[21]. Generally, any metal oxides absorption bands below 1000 cm^{-1} arise from interatomic vibrations^[22]. The strong absorption band at 974 cm^{-1} and 920 cm^{-1} indicated the stretching mode of $\text{Mo}=\text{O}$ ^[23]. The bands at 422 and 468 were assigned to vibration of $\text{Cu}-\text{O}$ bond^[24]. The bands at 830 and 879 cm^{-1} are assigned to vibration of CO_3^{2-} ^[25].

Scanning Electron Microscopy - Energy Dispersive X-Ray Spectroscopy (SEM-EDX)

The surface morphology and elemental composition were carried out by scanning electron microscope (SEM JEOL Japan make, 5610LV model) well equipped with an energy dispersive X-ray (EDAX) spectrophotometer and operated at 15 kV. The SEM image of $\text{Li}_2\text{CuMo}_2\text{O}_8$ is shown in Figure 3. It shows that the particles have not grown with uniform size.

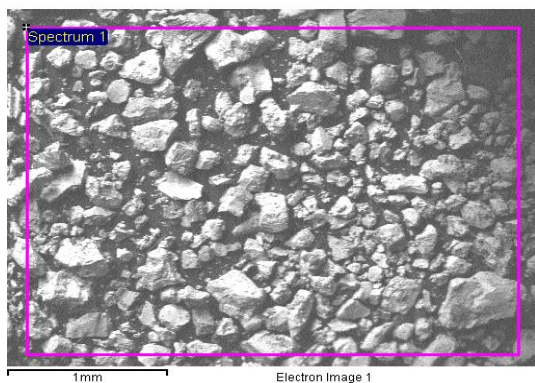


Figure 3: SEM of $\text{Li}_2\text{CuMo}_2\text{O}_8$

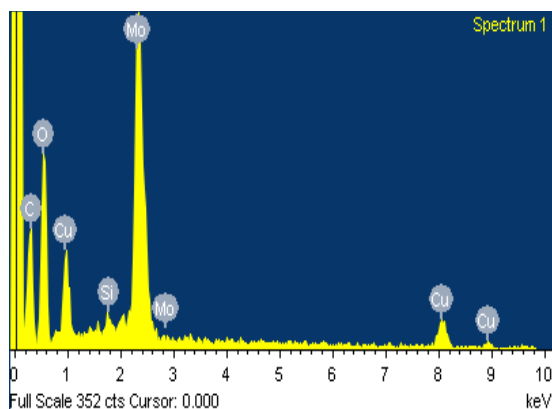


Figure 4: EDX of $\text{Li}_2\text{CuMo}_2\text{O}_8$

EDX analysis was performed to determine the elemental constituent of mixed Li-Cu-Mo oxide. Figure 4 reveals that four elements are present in the nanomaterial, i.e. Cu, Mo, C and O. The results are summarized in Table 1.

Table 1: Elemental composition

Elements	Weight%	Atomic%
C	29.67	50.69
O	3.086	39.58
Cu	9.53	3.08
Mo	29.46	6.30

Determination of lithium in a sample cannot be done as the electron energy involved is out of range of the detector. Thus, EDX results suggest that the values are in good agreement with the proposed formulae of $\text{Li}_2\text{CuMo}_2\text{O}_8$.

Results and Discussion

A solution of $3.6 \times 10^{-5}\text{ M}$ Azure A was prepared in doubly distilled water and 0.10g of lithium copper molybdate was added to it. The pH of the reaction mixture was adjusted to 10 and then this solution was exposed to a 200 W tungsten lamp at 50.0 mWcm^{-2} . It was observed that there was a decrease in the absorbance of the Azure A solution with increasing time of exposure. The plot of $\log A$ versus time was linear and hence, this reaction follows pseudo first-order kinetics. The rate constant (k) for this reaction was determined following the expression-

$$\text{Rate constant (k)} = 2.303 \times \text{slope} \quad \dots\dots (1)$$

The data of a typical run has been presented in Table 2 and graphically in Figure 5.

Table 2: A typical run

Time (min.)	Absorbance (A)	$1 + \log A$
0	0.523	0.718
15	0.430	0.633
30	0.357	0.552
45	0.285	0.454
60	0.241	0.382
75	0.205	0.311
90	0.188	0.274
105	0.174	0.240
120	0.152	0.181
135	0.146	0.164

pH = 10, Lithium copper molybdate = 0.10 g, [Azure A] = $3.6 \times 10^{-5}\text{ M}$, Light intensity = 50 mW cm^{-2}
Rate constant (k) = $2.47 \times 10^{-4}\text{ sec}^{-1}$

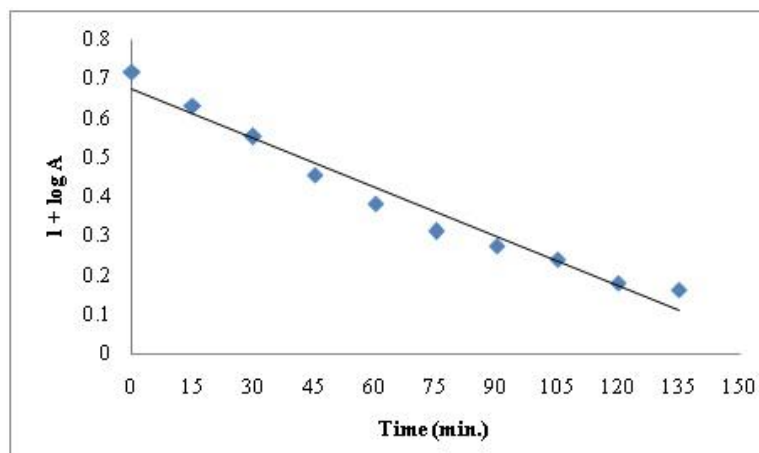


Figure 5: A typical run

Effect of pH

The effect of pH on photocatalytic degradation was investigated in the range 5.0- 10.5. The results are reported in Table 3.

Table 3: Effect of pH

pH	Rate constant (k) × 10 ⁴ (sec ⁻¹)
5.0	0.29
5.5	0.36
6.0	0.41
6.5	0.52
7.0	0.71
7.5	0.85
8.0	1.01
8.5	1.28
9.0	1.46
9.5	1.68
10.0	2.47

[Azure A] = 3.6 × 10⁻⁵ M, Light intensity = 50.0 mW cm⁻², Lithium copper molybdate = 0.10 g

It was observed that the rate of degradation of azure A increases on increasing pH regularly. All other variations have been made at pH 10 as the reaction becomes very fast on increasing pH of the reaction medium above 10. It may be due to the increasing attraction between cationic dye and negatively charged surface of the semiconductor, which increases as more and more OH⁻ ions are adsorbed on increasing pH of the reaction medium^[26].

Effect of Concentration of Azure A

The concentration of dye was varied from 3.1 × 10⁻⁵ to 4.0 × 10⁻⁵ M. the results are reported in Table 4.

It has been observed that the rate of photocatalytic degradation increases with an increase in the concentration of the dye up to 3.6 × 10⁻⁵ M. This may be due to the fact that as the concentration

of the azure A was increased, more dye molecules were available for excitation. Hence, an increased in the rate was observed. The rate of photocatalytic degradation was found to decrease with further increase in the concentration of dye. This may be attributed to the fact that the dye started acting as a filter for the incident light and it does not permit the desired light intensity to reach the photocatalyst surface in a limited time domain thus, decreasing the rate of photocatalytic degradation of azure A.^[27]

Table 4: Effect of dye concentration

[Azure A] × 10 ⁵ M	Rate constant (k) × 10 ⁴ (sec ⁻¹)
3.1	0.46
3.2	0.92
3.3	1.19
3.4	1.28
3.5	1.68
3.6	2.47
3.7	2.22
3.8	2.06
3.9	1.96
4.0	1.85

pH = 10.0, Light intensity = 50.0 mW cm⁻², Lithium copper molybdate = 0.10 g

Effect of the Amount of Photocatalyst

The effect of the amount of photocatalyst is also likely to affect the process of dye degradation and therefore, different amounts of photocatalyst were used. The results are reported in Table 5.

The rate of reaction was found to increase on increasing the amount of semiconductor, lithium copper molybdate. The rate of degradation reached to its optimum value at 0.10 g of the photocatalyst. Beyond 0.10g, the rate of reaction becomes almost constant. This may be explained on the basis that as the amount of semiconductor was increased, the exposed surface area of the semiconductor was

increased. However, after a particular value (0.10 g), an increase in the amount of semiconductor will only increase the thickness of layer of the semiconductor and not its exposed surface area^[28].

Table 5: Effect of lithium copper molybdate

Lithium copper molybdate (g)	Rate constant (k) × 10 ⁴ (sec ⁻¹)
0.02	1.86
0.04	1.98
0.06	2.12
0.08	2.21
0.10	2.47
0.12	2.16
0.14	2.15
0.16	2.14

pH = 10.0, Light intensity = 50.0 mW cm⁻², [Azure A] = 3.6 × 10⁻⁵ M

Effect of Light Intensity

The effect of the variation of the light intensity on the rate was also investigated and the results are reported in Table 6.

The data indicate that photocatalytic degradation of azure A was enhanced with the increase in intensity of light, because an increase in the light intensity will increase the number of photons striking per unit area per unit time of photocatalyst surface.

Table 6: Effect of light intensity

Light intensity (mW cm ⁻²)	Rate constant (k) × 10 ⁴ (sec ⁻¹)
20.0	0.54
30.0	1.27
40.0	1.95
50.0	2.47
60.0	2.28
70.0	2.16

pH = 10, Lithium copper molybdate = 0.10 g, [Azure A] = 3.6 × 10⁻⁵ M

There was a slight decrease in the rate of reaction as the intensity of light was increased beyond 50.0 mW cm⁻². Therefore, light intensity of medium over was used throughout the experiments.²⁹

Determination of Water Quality Parameters

Quality of water before and after photocatalytic degradation has been tested by measuring some parameters and results are summarized in Table 7.

Table 7: Water quality parameters

Parameter	Before photocatalytic degradation	After photocatalytic degradation
pH	10.0	8.2
Conductivity(μS)	780	891
TDS (ppm)	522	596
Salinity (ppt)	0.65	0.72
DO (ppm)	10.4	15.2
COD (mg/L)	50	30

pH

pH of sample represents the extent of its pollution by acidic and alkaline wastes. All chemical and biological reactions directly depend upon the pH of medium. pH of azure A is basic in range before the degradation but after the photocatalytic degradation of the dye, pH reaches to near neutral range. It is clear that photocatalytic treatment affects the pH and makes it more desirable. pH of dye solution is not in permissible limit and is not suitable for irrigation and drinking purpose according to WHO standard, whereas pH of photocatalytically treated water by Li₂CuMo₂O₈ is suitable for animal and aquatic biota. This result indicates that pH value of sample is in slightly alkaline range but within the ISI permissible limits^[30].

Conductivity

Conductivity, as summation parameters is measure of the level of ion concentration of a solution. It is directly proportional to its dissolved mineral matter content. Consequently it is an index of the salt load in waste water or the purity of water, Conductivity is only a quantitative measurement. Only ionizable material will contribute to conductivity. Conductivity was found to be increased in treated water. Slight decrease in pH and increase in conductivity also confirms the mineralization of dye into CO₂ and inorganic ions such as CO₃²⁻, NO₃⁻, SO₄²⁻, etc.

Total dissolved solid (TDS) and Salinity

Dissolved solids refer to any mineral, salt, metal cation, or anion dissolved in water. This includes anything present in water other than pure water molecules and suspended solids. In general, the high TDS result in an undesirable taste, which could be salty, bitter or metallic. It could also give gastrointestinal irritation. TDS value of azure A increased from 522 ppm to 596 ppm due to mineralization of dye particles.

Dissolved oxygen (DO)

Dissolved oxygen indicates physical and biological activity in water. The minimum standard limit is 5 ppm. Oxygen can serve as electron sink to trap the excited conduction band electron from reactive oxygen species. DO is proposed to be

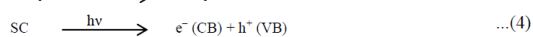
responsible cleavage of aromatic ring of dye molecule. Value of azure a dye increased from 10.4 to 15.2 ppm^[31].

Chemical oxygen demand (COD)

The chemical oxygen demand is widely used as an effective data to measure the organic strength of wastewater. This test allows the measurement of waste in terms of the total quantity of oxygen required for the oxidation of organic matter to CO₂ and water. The COD of the dye solution before and after the treatment was estimated. The reduction in COD values of the treated dye solution indicates the mineralization of dye molecules along the colour removal^[32].

Mechanism

On the basis of our experimental observation, a tentative mechanism for photocatalytic degradation of Azure A may be proposed as:



Azure A absorbs radiations of desired wavelength and it is excited giving its first excited singlet state. Further, it undergoes intersystem crossing (ISC) to give its more stable triplet state. Along with this, the semiconducting lithium copper molybdate (SC) also utilizes this energy to excite its electron from valence band to the conduction band. An electron can be absorbed from hydroxyl ion by hole (h⁺) present in the valence band of semiconductor generating $\bullet\text{OH}$ radical. This hydroxyl radical will oxidize azure A to its leuco form, which may ultimately degrade to products. It was confirmed that the $\bullet\text{OH}$ radical participates as an active oxidizing species in the mineralization of azure A as the rate of degradation was appreciably reduced in presence of hydroxyl radical scavenger (2-propanol). The presence of SO₄²⁻, and NO₃⁻ ions were confirmed by their usual chemical tests. Carbon dioxide and water were major products of degradation.

Conclusion

The feasibility of photocatalytic degradation of azure a dye was tested using synthesized Li₂CuMo₂O₈ semiconductor as photocatalyst. The experimental results indicated that degradation efficiency of azure A was affected by pH, concentration of dye, amount of semiconductor and light intensity. It was observed that photocatalytic treatment increased the biodegradability of dye

containing polluted water. It helps to reduce pH, COD. It also increases DO, TDS, salinity and conductivity. In the present work, a quaternary semiconductor lithium copper molybdate was successfully used as a photocatalyst for degradation of azure A. It may be explored for removal of a variety of industrial effluents in future.

References

1. Kansal S.K., and Singh M., Studies on photodegradation of two commercial dyes in aqueous phase using different photocatalysts, *J. Hazard. Mater.*, **141(3)**, 581(2007)
2. Chakrabarti S., and Dutta B.K., Photocatalytic degradation of model textile dyes in wastewater using ZnO as semiconductor catalyst, *J. Hazard. Mater.*, **112(3)**, 269(2004)
3. Tabatabaei S.M., Dasmalchi S., Mehrizad A., Gharbani P., Enhancement of 4-nitrophenol ozonation in water by nano ZnO catalyst, *Iran. J. Environ. Health Sci. Eng.*, **8(4)**, 363 (2011)
4. Pardeshi S.K., and Patil A.B., A simple route for photocatalytic degradation of phenol in aqueous zinc oxide suspension using solar energy, *Solar Energy*, **82(8)**, 700(2008)
5. Ali R., Baker W.A.W.A., and Teck L.K., Zn/ZnO/TiO₂ and Al/Al₂O₃/TiO₂ photocatalysts for the degradation of cypermethrin, *Mod. Appl. Sci.*, **4(1)**, 59(2010)
6. Zhang S., Li J., Niu H., Xu W., Xu J., Hu W. and Wang X., Visible-light photocatalytic degradation of methylene blue using SnO₂/α-Fe₂O₃ hierarchical nanostructures, *Chem. Phys. Chem.*, **78(2)**, 192 (2013)
7. Kale B., Baeg J., Yoo J.S., Lee S.M., Lee C.W., Moon S., Chang H., Synthesis of a novel photocatalyst, ZnBiVO₄, for the photodecomposition of H₂S, *Canad. J. Chem.*, **83(6-7)**, 527(2005)
8. Chen, L., Zhang S., Wang L., Xue D., Preparation and photocatalytic properties of strontium titanate powder via sol-gel process, *J. Cryst. Growth.*, **311(3)**, 746 (2009)
9. Bhati I., Punjabi P.B., and Ameta S.C., Photocatalytic degradation of fast green using nanosized CeCrO₃, Macedonian, *J. Chem. Chem. Eng.*, **29(2)**, 195 (2010)
10. Huang C. M., Huang L. S., Li Y. S., Liu I. H., and Chang C. Y., Photocatalytic degradation and mineralization of gaseous isopropanol over silver vanadates, *Sustain. Environ. Res.*, **21(1)**, 45 (2011)

11. Ameta R., Sharma D., Ordia M., Photocatalytic degradation of crystal violet using nickel containing polytungstometalate, *Sci. Revs. Chem. Commun.*, **3**(2), 2277 (2013)
12. Ghorai T. K., and Biswas N., Photodegradation of rhodamine 6G in aqueous solutions via SrCrO₄ and TiO₂ nano- sphere mixed oxide, *Mater. Res. Technol.*, **2**(1), 10 (2013)
13. Mahata P., Aarthi T., Madras G., Natarajan S., Photocatalytic degradation of dyes and organics with nanosized GdCoO₃, *J. Phys. Chem. C.*, **111**(4),1665(2007)
14. Sadiq J.M., Nesaraj S.A., Development of NiO-Co₃O₄ nano- ceramic composite materials as novel photocatalysts to degrade organic contaminants present in water, *Int. J. Environ. Res.*,**8**(4),1171 (2014)
15. Liu H., Chen Z., Jin Z., Su Y., and Wang Y., A reduced graphene oxide supported Cu₃SnS₄ composite as an efficient visible-light photocatalyst, *J. Chem. Soc. Dalton Trans.*, **43**,7491(2014)
16. Zhao X., Xu T., Yao W., Zhu Y., Photodegradation of dye pollutants catalyzed by g-Bi₂MoO₆ nanoplate under visible light irradiation, *Appl. Surf. Sci.*, **255**, 8036 (2009)
17. Aslam I.,Cao C., Farooq M. H., Khan W. S., Tahir M., Idrees F.,Khalid S., A novel Z-scheme WO₃/CdWO₄ photocatalyst with enhanced visible-light photocatalytic activity for the degradation of organic pollutants, *RSC Adv.*, **5**, 6019(2015)
18. Chen C., Wang Q., Lei P., Song W., Ma W.,and Zhao J., Photodegradation of dye pollutants catalyzed by porous K₃PW₁₂O₄₀ under visible light irradiation, *Environ. Sci. Technol.*, **40**(12), 3965 (2006)
19. Clark J.H., Dyer M.S., Palgrave R.G., Ireland C.P., Darwent J.R., Claridge J.B., Rosseinsky M.J., Visible light photo-oxidation of model pollutants using CaCu₃Ti₄O₁₂ : An experimental and theoretical study of optical properties, electronic structure, and selectivity, *J. Am. Chem. Soc.*, **133**, 1016 (2011)
20. Luan J., Pan B., Paz Y., Li Y., Wu X., and Zou Z., Structural, photophysical and photocatalytic properties of new Bi₂GaVO₇ under visible light irradiation, *Phys. Chem. Chem. Phys.*, **11**, 6289(2009)
21. Sujana M. G., and Anand S., Iron and aluminium based mixed hydroxides: A novel sorbents for fluoride removal from aqueous solution, *J. Appl. Surf. Sci.*,**256**, 6956 (2010)
22. Wachs I. E., Physicochemical and engineering aspect, *Coll. Surf.*,**105**, 143 (1995)
23. Irmawati R. and Shafizah M., The production of high purity hexagonal MoO₃ through the acid washing of as-prepared solids, *Inter. J. Basic Appl. Sci.*,**9**, 34 (2009)
24. Kannaki K., Ramesh P.S., and Geetha D., Hydrothermal synthesis of CuO nanostructure and their characterizations, *Inter. J. Sci. Engg. Res.*,**3**, 1 (2012)
25. Choi Y.-K., Chung K. I., Kim W.-S., Sung Y.-E., and Park S.-M., Suppressive effect of Li₂CO₃ on initial irreversibility at carbon anode in Li-ion batteries, *J. Power Sources*,**104**,132 (2002)
26. Ameta R., Verdia J., Punjabi P. B., and Ameta S. C., Use of semiconducting iron(III) oxide in photocatalytic bleaching of some dyes, *Indian J. Chem. Technol.*,**13**, 114 (2006)
27. Bhati I., Punjabi P. B., and Ameta S.C., Photocatalytic degradation of fast green using nanosized CeCrO₃,*Maced. J. Chem. Chem. Eng.*,**29**, 195 (2010)
28. Ameta A., Ameta R., and Ahuja M., Role of ferric tungstate as photocatalyst for removal of xylenol orange, *Acta Chem. Pharm. Indica*, **3**, 268 (2013)
29. Chanderia K., Kalal S., Sharma J., Ameta N., and Punjabi P. B., Heterogeneous photo-Fenton like degradation of rhodamine B using copper loaded bentonite and H₂O₂, *Indian J. Chem.*,**52**(A),1416 (2013)
30. Tiwari R., Sharma M.K., and Ameta S.C., Photocatalytic treatment of polluted water containing cresol red, *Int. J. Chem. Sci.*, **9**, 421 (2011)
31. Jakar S., Chaturvedi R., and Sharma M.K., Comparison of efficiency of APM and MnO₂ by photocatalytic degradation of saranine-o based on quality parameter modification, *Harmoniz. Res. Appl. Sci.*,**2**, 241, (2014)
32. Byrappa K., Subramani A.K., Ananda S., Lokanatha Rai K.M., Dinesh R., and Yashimura M., Photocatalytic degradation of rhodamine B dye using hydrothermally synthesized ZnO, *Bull. Mater. Sci.*, **29**, 433(2006).